Article

Dynamic Monitoring of Environmental Quality in the Loess Plateau from 2000 to 2020 Using the Google Earth Engine Platform and the Remote Sensing Ecological Index

Jing Zhang [1], Guijun Yang [1,2,*], Liping Yang [1], Zhenhong Li [1], Meiling Gao [1], Chen Yu [1], Enjun Gong [3], Huiling Long [2] and Haitang Hu [2]

[1] School of Geological Engineering and Geomatics, Chang'an University, Xi'an 710054, China
[2] Key Laboratory of Quantitative Remote Sensing in Agriculture of Ministry of Agriculture and Rural Affairs, Information Technology Research Center, Beijing Academy of Agriculture and Forestry Sciences, Beijing 100097, China
[3] College of Surveying and Geo-Informatics, North China University of Water Resources and Electric Power, Zhengzhou 450045, China
*   Correspondence: yanggj@nercita.org.cn

Abstract: The Loess Plateau is a typical ecologically sensitive area that can easily be perturbed by the effects of human activities and global climate change. Therefore, it is necessary to develop tools to monitor the environmental quality in the LP quickly and accurately. To reveal the spatio-temporal changes in environmental quality in the LP from 2000 to 2020, we used the Moderate-Resolution Imaging Spectroradiometer (MODIS) products on the Google Earth Engine platform and constructed the remote sensing ecological index (RSEI) through principal component analysis (PCA). Then, Sen–Mann–Kendall methods were applied to determine the changing trend of the environmental quality of the LP. Finally, natural and anthropogenic factors affecting the environmental quality were probed using a geographical detector model. The results showed that: (1) the average RSEI values in 2000, 2010 and 2020 were 0.396, 0.468 and 0.511, respectively, displaying an upward trend from 2000 to 2020, with a growth rate of 0.005 year^{-1}. The overall environment quality was moderate (0.4–0.6). (2) In terms of spatial distribution, the environmental quality was excellent in the southeast and poor in the northwest of the LP. The areas with improved environmental quality (84.51%) were located in all the counties, whereas the areas with degraded environmental quality (8.11%) occurred in the north and southeast of the study area. (3) Greenness, heat, wetness, dryness and land use types were prominent factors affecting RSEI throughout the study period; additionally, the total industrial gross domestic product showed a growing influence. The contribution of multi-factor interaction was stronger than that of single factors. The results will provide a reference and a new research perspective for local environmental protection and regional planning.

Keywords: remote sensing ecological index; Google Earth Engine; trend analysis; geographic detector; the Loess Plateau

1. Introduction

The eco-environment is defined as "the total amount and quality of water resources, land resources, biological resources and climate resources that affect human survival and development", and it is an indispensable element for human survival [1]. However, the acceleration of urbanization and the rapid growth of the population have caused the excessive consumption of natural resources [2], leading to substantial ecosystem disturbances at various scales [3]. This disturbance has seriously damaged the ecological balance and has threatened human existence [4]. Therefore, the demand for environmental quality assessments has gradually increased.

As an important ecological screen in Northwestern China, in recent years, the LP has experienced a slew of environmental issues, including severe soil erosion, enormous

environmental pressure and degraded ecosystem service function [5,6]. Thus, it is urgent to implement environmental conservation measures that can protect this ecologically fragile region. National environmental protection policies, large-scale land restoration projects and ecological construction projects have been implemented in this region since the 1970s [7]. For example, the Grain for Green Project was launched in 1999, aiming to reduce soil erosion and desertification by converting 14.67 million hectares of farmland to forest by 2010 (of which 4.4 million hectares were on land with a slope greater than 25°) [6]. In 2006, the Chinese government carried out an essential national ecological security strategic pattern construction plan—the national barrier zone [8]. This scheme aimed to improve the stability of ecosystems and reduce environmental stress. In 2007, the concept or idea of "ecological civilization" was further stressed by the Chinese government and written into China's "13th Five-year Plan" (2016–2020), promoting environmental protection and restoration [9]. In 2018, the Chinese government issued a "Work Plan of poverty Alleviation" aimed at developing an ecological industry [10]. Thus far, the implementation of these actions has exerted a positive impact on environmental quality. However, the LP is still one of the most ecologically fragile areas due to frequent natural disasters [11]. In addition, the region is faced with long-term soil erosion, drought and water shortage problems [12]. Therefore, scientific and efficient evaluation of the environmental quality of the spatiotemporal evolution law has become an urgent issue in this region, which is of great significance to environmental protection and sustainable development in the LP.

With the advantages of convenient and low-cost data acquisition and continuous land surface information coverage, remote sensing technology provides a new technical means for studying environmental quality [13]. At present, environmental quality evaluation models can be divided into two types. One type mainly applies a single ecological indicator (Normalized Difference Vegetation Index (NDVI) [14], Enhanced Vegetation Index (EVI) [15], Land surface Temperature (LST) [16]) and is used more widely in the early stages. Due to the complexity of natural systems, it is difficult to accurately and comprehensively characterize the ecological status by only a single ecological indicator [17]. Therefore, a model integrating multiple indicators to evaluate the ecological status was gradually proposed. In 2006, the Ministry of Environmental Protection of China issued the Ecological Environment Index (EI) in the Technical Specifications for Ecological Environment Status Assessment (HJ/T192-2006), which has been widely used in the field of environmental research. Francois et al. [18] combined NDVI and Microwave Polarization Difference Index (MPDI) for monitoring the relative sensitivity of vegetation and desertification. Khan et al. [19] integrated NDVI and LST for drought monitoring in Punjab, Pakistan, based on 12 indicators, including average precipitation, altitude, biomass abundance index, net primary productivity, and industrial wastewater discharge. Chang et al. [20] constructed a conceptual framework to quantitatively evaluate the environmental quality of the upper reaches of the Hanjiang River in Shaanxi Province. However, the above methods are greatly affected by subjective factors and are based mostly on annual statistical data, meaning that they cannot be rapidly updated. Moreover, it is difficult to obtain detailed characteristics of environmental quality on the basis of annual statistical data. Therefore, Xu et al. [21] extracted greenness, heat, dryness and wetness indicators and constructed a remote sensing ecological index (RSEI) based on principal component analysis (PCA). These comprehensive evaluation methods mostly adopt the fuzzy evaluation method [22], the analytic hierarchy process (AHP) [23] and PCA method. The fuzzy evaluation method is mainly used to solve the problem of uncertain influencing factors, but relies on the subjective judgment of the decision maker, making it difficult to consider the objectivity of the actual problem [24]. Compared with the fuzzy evaluation method, AHP combines qualitative judgment with quantitative inference, but it is still a semi-quantitative method, which reduces the credibility of the results [25]. PCA can automatically allocate the weight of each factor according to data characteristics, improving the reliability of the results. Therefore, RSEI has been applied and verified at different regional scales due to its advan-

tages of convenient index acquisition and strong reliability. For example, at the local scale, Sukamal et al. [26] and Qureshi et al. [27] evaluated the environmental quality of Kolkata City cluster in India and Gomishan wetland in Iran, respectively. At the regional scale, Ji et al. [2] tracked a long time series of ecological condition changes in China based on RSEI. However, traditional methods have low processing efficiency when facing a large region or a large amount of data. As an effective tool for processing massive information, the Google Earth Engine (GEE) cloud platform can efficiently access and process a large amount of data sets, providing an effective way to solve this problem [28]. Yang et al. [29] used MODIS product image sets to explore spatio-temporal changes of environmental quality based on the GEE cloud platform and then comprehensively analyzed their relationship with topographic environmental factors in the Yangtze River Basin from 2001 to 2019.

Trend analysis is also an important component of an environmental assessment. At present, three main types of trend analysis approaches are adopted, namely linear regression analysis, Theil-Sen slope estimation [30] and Mann–Kendall (MK) trend analysis [31,32]. Although linear regression analysis is widely utilized, it is sensitive to numerical distribution, which requires the data to conform to the normal distribution and has poor resistance to outliers [33]. Theil–Sen slope estimation and MK analysis have good robustness and are not affected by outliers. Their combination could be used to analyze the change trend of environmental quality and perform significant tests, which have certain advantages compared with simple linear regression [34], drawing the attention of numerous researchers.

In recent years, the severe ecological issues of the LP have drawn widespread attention from scholars. Lü et al. [35] studied the changes in ecosystem services such as water regulation and soil conservation in the LP. Su et al. [8] combined meteorological, soil and hydrological data to explore the spatio-temporal changes and driving forces of the ecosystem in the LP region. Xiao et al. [36] carried out a comprehensive evaluation between social economy and ecological environment based on the coupling coordination degree in the LP. However, most previous studies have focused on ecosystem services, and although some studies have examined ecosystem driving forces in the LP, the interaction between natural and socioeconomic factors on environmental quality remains unclear. In addition, it is necessary to study the optimal range of drivers of RSEI change in the LP, which can help us identify the conditions needed for preserving the environment. Therefore, analyzing the change trend and driving mechanism of environmental quality in the LP can provide the scientific basis for the management of the environment.

In view of the above research background, this study aimed to: (1) calculate the indicators NDVI, LST, Wetness (WET), and Normalized Differential Building–Soil Index (NDBSI) to construct RSEI using the PCA method to analyze the spatio-temporal change characteristics of environmental quality in the LP from 2000 to 2020, (2) analyze the areas of improvement and degradation of environmental quality by using the Theil–Sen–MK method, (3) and explore the driving mechanism of environmental quality change in the LP.

2. Study Area

The LP (Figure 1) is located in the northern part of central China (33°43′N–41°16′N, 100°54′E–114°33′E), covering the areas of Shanxi, Ningxia and parts of Shaanxi, Qinghai, Henan and Gansu provinces and Inner Mongolia. It covers an area of 640,000 km², accounting for about 6.7% of China's land area [36]. The terrain is high in the northwest and low in the southeast, with an elevation of about 1500–2000 m. This region is dominated by an arid and semi-arid climate with mean annual precipitation of 200–700 mm and an annual average temperature ranging from 9 to 12 °C [37]. The precipitation gradually decreases from southeast to northwest and is mostly concentrated from June to September. Soil erosion leads to typical ecological fragility in LP.
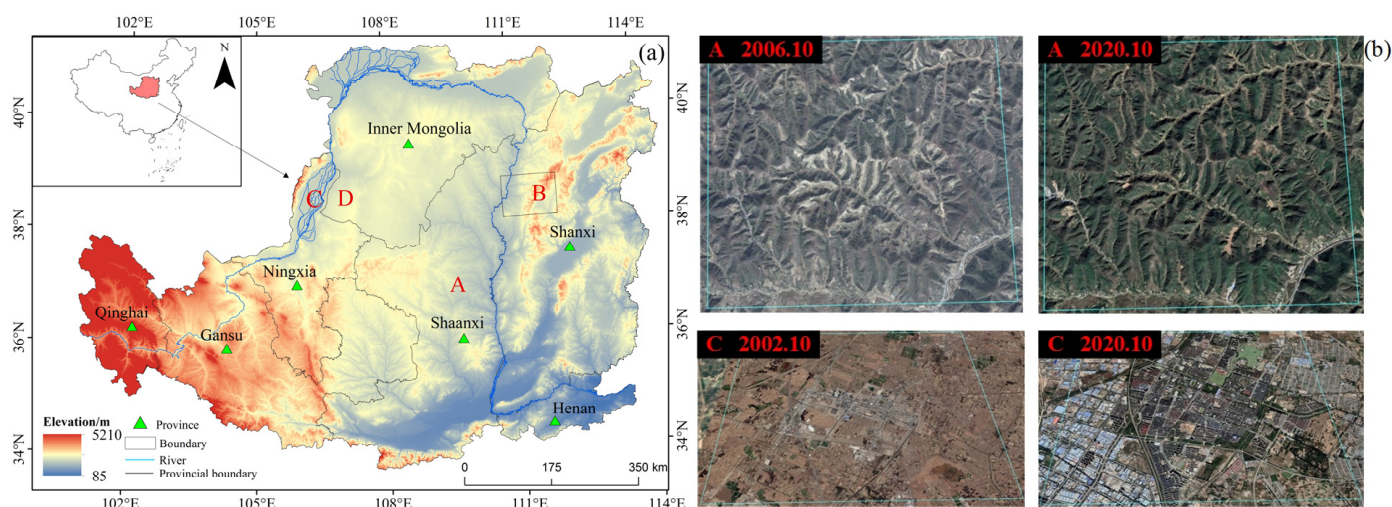
Figure 1. Location of the study area. A and B show an increase in vegetation after the Grain for Green Project, while C and D show the expansion of cities in (**a**) and A and C are from Google Earth satellite images in (**b**), and B and D are for subsequent analysis.

3. Data and Methods

3.1. Data Sources and Processing

Based on GEE, MODIS products from May to October in 2000, 2010 and 2020 were screened as the main remote sensing data to construct the RSEI. The specific description of the products is shown in Table 1. The elevation data were from the Shuttle Radar Topography Mission (SRTM) DEM with a spatial resolution of 30 m; the slope was extracted from DEM. Socioeconomic statistics data were derived from Shanxi, Ningxia, Shaanxi, Qinghai, Henan, Gansu and Inner Mongolia Statistical Yearbook 2000 to 2020, including the gross industrial product (GDP) and the gross output value of agriculture, forestry, animal husbandry and fishery. The population density data were from the World's Population Grid (GPWv4.11) data set (https://sedac.ciesin.columbia.edu (accessed on accessed on 16 March 2022)). The land use data of the LP in 2000, 2010 and 2020 were derived from the GlobeLand30 maps (30 m) provided by the National Geomatics Centers of China (http://www.globallandcover.com (accessed on accessed on 16 March 2022)).

Table 1. Indicators and data description.

Indicators	Product	Spatial Resolution (m)	Temporal Resolution (d)	Number of Scenes	Data Level	Years
NDVI	MOD13A1	500	16	30	L3	2000, 2010, 2020
LST	MOD11A2	1000	8	61	L3	2000, 2010, 2020
WET/NDBSI	MOD09A1	500	8	61	L2	2000, 2010, 2020

3.2. Research Methods

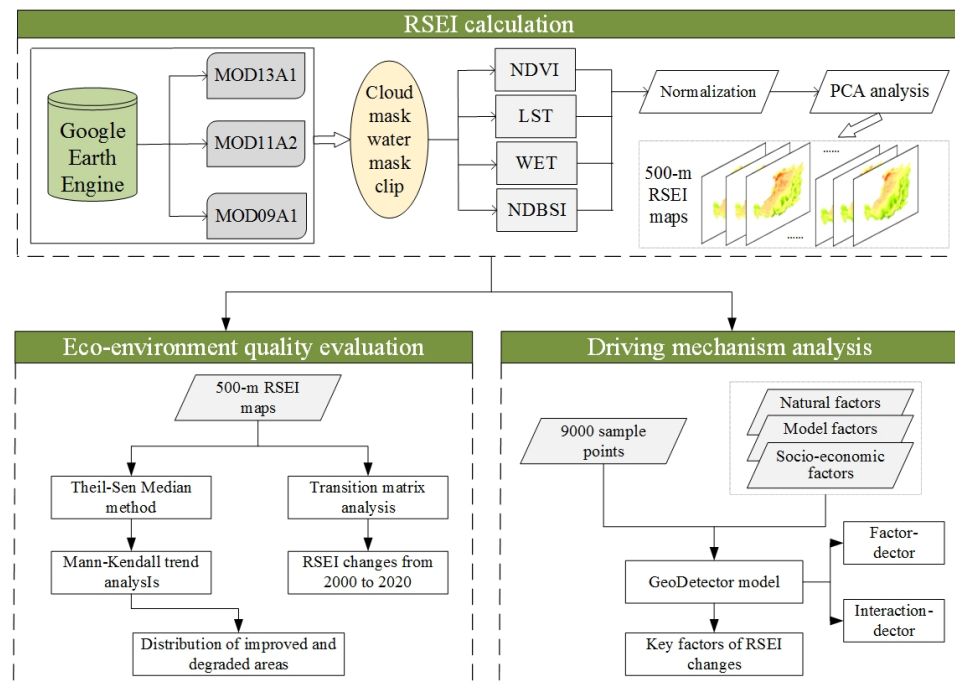Figure 2 presents the framework of this study.

Figure 2. Technology flowchart.

3.2.1. Calculation of RSEI

(1)   Normalized difference vegetation index

As an effective indicator to reflect vegetation growth, NDVI has been widely used to monitor seasonal, interannual and long-term changes of vegetation structure, phenology and biophysical parameters [38]. It can be calculated as [18]:

$$\text{NDVI} = \frac{\rho_{nir} - \rho_{red}}{\rho_{nir} + \rho_{red}} \tag{1}$$

where ρ_{nir}, ρ_{red} denote the reflectance of the near-infrared (NIR1) and red bands in MODIS data, respectively.

(2)   LST

LST is an important indicator affecting vegetation growth and environmental change [39]. It was acquired from MOD11A2 by converting daytime surface temperature data into actual surface temperature on the GEE using the following formula:

$$\text{LST} = 0.02 \times \text{DN} - 273.15 \tag{2}$$

where DN is the gray value of land surface temperature.

(3)   Wetness

The wetness indicator (WET) obtained from the MOD09A1 product based on tasseled cap transformation effectively reflects the humidity status of vegetation, water and soil [40], and the formula is expressed as [41]:

$$\text{WET} = 0.1147\rho_{red} + 0.2489\rho_{nir1} + 0.2408\rho_{blue} + 0.3132\rho_{green} - 0.3122\rho_{nir2} - 0.6416\rho_{swir1} - 0.5087\rho_{swir2} \tag{3}$$

where ρ_{red}, ρ_{nir1}, ρ_{blue}, ρ_{green}, ρ_{nir2}, ρ_{swir1}, and ρ_{swir2} denote the reflectance of the red, NIR1, blue, green, NIR2, short-wavelength infrared 1 (SWIR1), and SWIR2 bands in the MODIS data, respectively.

(4) Normalized differential build-up and bare soil index

The NDBSI, which reflects the damage to natural landscapes caused by the rapid expansion of building land and bare soil exposure, is computed by the Index-based Built-up Index (IBI) [42] and Soil Index (SI) [43]. The calculation formula of each indicator is expressed as [42,43]:

$$NDBSI = \frac{IBI + SI}{2} \tag{4}$$

$$SI = \frac{(\rho_{swir1} + \rho_{red}) - (\rho_{nir} + \rho_{blue})}{(\rho_{swir1} + \rho_{red}) + (\rho_{nir} + \rho_{blue})} \tag{5}$$

$$IBI = \frac{\frac{2\,\rho_{swir1}}{\rho_{swir1} + \rho_{nir}} - \left[\frac{\rho_{nir}}{\rho_{nir} + \rho_{red}} + \frac{\rho_{green}}{\rho_{green} + \rho_{swir1}}\right]}{\frac{2\,\rho_{swir1}}{\rho_{swir1} + \rho_{nir}} + \left[\frac{\rho_{nir}}{\rho_{nir} + \rho_{red}} + \frac{\rho_{green}}{\rho_{green} + \rho_{swir1}}\right]} \tag{6}$$

where ρ_{swir1}, ρ_{red}, ρ_{nir}, ρ_{blue}, and ρ_{green} denote the reflectance of SWIR1, red, NIR, blue, and green bands in the MODIS data, respectively.

(5) Normalization of the Measures

Due to the different units and numerical range of each indicator, the four indicators were normalized using the following formula:

$$NI_i = \frac{I_i - I_{min}}{I_{max} - I_{min}} \tag{7}$$

where NI_i represents the normalized value of an indicator, I_i denotes the index value, I_{min} and I_{max} correspond to the minimum and maximum values, respectively.

The four indicators NDVI, LST, WET, and NDBSI were used to represent greenness, heat, wetness, and dryness, respectively. The above indicators were coupled by PCA; then, PC1 was used to build the RSEI:

$$RSEI_0 = 1 - PC1[f(NDVI, LST, WET, NDBSI)] \tag{8}$$

In addition, RSEI was normalized based on $RSEI_0$ according to Equation (7).

3.2.2. RSEI Trend Analysis

Theil–Sen Median, a robust linear non-parametric method, does not need data to conform to a specific distribution and removes the interference of outliers. It has become an important method for evaluating the trend of long-term series [34]. The calculation formula is [30]:

$$\beta = \text{median}\frac{RSEI_j - RSEI_i}{j - i}, \ 2000 \ll i \le j \le 2020 \tag{9}$$

where $RSEI_i$, $RSEI_j$ represent RSEI values at year i and j, respectively. When $\beta > 0$, there is an improvement trend. When $\beta < 0$, there is a degradation trend.

The Mann–Kendall (MK) test was used to perform the significance test. The statistical value Z was calculated as [31,32]:

$$S = \sum_{i=1}^{n-1} \sum_{j=i+1}^{n} \text{sign}(RSEI_j - RSEI_i) \tag{10}$$

$$\text{sign}(RSEI_j - RSEI_i) = \begin{cases} +1 & RSEI_j - RSEI_i > 0 \\ 0 & RSEI_j - RSEI_i = 0 \\ -1 & RSEI_j - RSEI_i < 0 \end{cases} \tag{11}$$

$$Z = \begin{cases} (S-1)/\sqrt{\text{var}(S)} & S > 0 \\ 0 & S = 0 \\ (S+1)/\sqrt{\text{var}(S)} & S < 0 \end{cases} \tag{12}$$

where var is the variance, and n is the length of time series. In this paper, the significance test was carried out at the significance level $\alpha = 0.05$. When $|Z| > 1.96$, the trend is significant; otherwise, it is non-significant.

3.2.3. Analysis of Driving Forces Based on Geographic Detector

The geographic detector model is a statistical method used to detect the spatial heterogeneity of the dependent variable Y and to reveal the driving forces behind it [44]. It mainly includes factor detector, risk detector, ecological detector and interaction detector. This study used the factor detector to quantify the influence of independent variable X on the spatial distribution of RSEI, which can be expressed by the q value. The calculation formula is as follows [44]:

$$q = 1 - \frac{\sum_{h=1}^{L} N_h \sigma_h^2}{N \sigma^2} \tag{13}$$

where q measures the explanatory power of driving factors on RSEI; $q \in [0, 1]$. A larger q value indicates a more powerful influence of the factor on RSEI. L represents the stratification of the dependent variable RSEI or factor X; N_h, δ_h^2 denote the number of units and variance of layer h, respectively; N, σ^2 represent the number of units and variance of the study, respectively.

The risk detector was used to examine whether there was a significant difference in the mean value of attributes between two sub-regions with the t statistic. The interaction detection was used to identify the interaction of different influencing factors on RSEI. Natural factors and terrain conditions are always the basic factors affecting environmental quality [45]. In addition, local land-use and land-cover change play a key role in ecological change [46]. Thus, land use types, elevation and slope were used as natural factors. Studies have confirmed that human activities such as inappropriate land use lead to serious ecological problems [47], and the impact of economic development and population growth on the environment cannot be ignored [47,48]. Population and GDP are important human disturbance factors [49]. Considering the availability, representativeness and credibility of indicators, population density, GDP and gross output value of agriculture, forestry, animal husbandry and fishery at district or county levels were selected as socio-economic factors. Xia et al. [50] revealed the NDVI, LST, WET and NDBSI factors for the changes in the RSEI. Therefore, it is necessary to study the influence of these factors as model factors on RSEI in our study (Table 2). Following, 9000 sampling points at 3×3 km were randomly generated using ArcGIS10.6. Then, the corresponding attribute values of the RSEI and factors were read into the geo-detector software. The natural breakpoint method was selected to divide the factors into groups and to classify the data according to their intrinsic properties, reducing the variance within groups and increasing the variance between groups [51].

Table 2. Driving factors of environmental quality.

Factor Types	Driving Factors	Factor Symbols	Unit	Type Numbers
Socioeconomic factors	Population density	X1	people/ km^2	8
	Gross domestic product (GDP)	X2	Hundred million yuan	10
	Gross output value of farming, forest, animal husbandry and fishery	X3	Hundred million yuan	10
Natural Factors	Land use types	X4	—	9
	Elevation	X5	m	8
	Slope	X6	°	8
Model factors	NDVI	X7	—	8
	LST	X8	—	8
	WET	X9	—	8
	NDBSI	X10	—	8

4. Results

4.1. Spatio-Temporal Variations Analysis of RSEI

4.1.1. PCA Analysis of RSEI Indicators

In this paper, the RSEI from 2000 to 2020 in the LP was constructed through the PCA on the GEE platform. The contribution rate of the first principal component (PC1) reached 86.81%, 89.09% and 87.57% in 2000, 2010 and 2020, respectively, indicating that PC1 had concentrated the most characteristic information of the four indicators (Table 3). Thus, it was reasonable to construct RSEI using PC1, which expressed the regional environmental quality. In PC1, the eigenvalues of NDVI and WET were positive, indicating that they had positive ecological benefits. In contrast, the NDBSI and LST were negative, indicating that they had negative ecological benefits, which was consistent with the actual situation.

Table 3. Results of principal component (PC) analysis.

Year	Indicators	PC1	PC2	PC3	PC4
2000	NDVI	0.6274	0.4617	0.4051	−0.4785
	LST	−0.3535	−0.4160	0.8203	−0.1703
	WET	0.4513	−0.7636	−0.2704	−0.3740
	NDBSI	−0.5269	0.1747	−0.2996	−0.7759
	Eigenvalue	0.0691	0.0053	0.0040	0.0012
	Percent eigenvalue (%)	86.8091	6.6583	5.0251	1.5075
2010	NDVI	0.5772	0.4744	−0.3917	−0.5368
	LST	−0.3362	0.7206	0.5867	−0.1528
	WET	0.4248	−0.4377	0.6717	−0.4203
	NDBSI	−0.6109	−0.2527	−0.2259	−0.7154
	Eigenvalue	0.0866	0.0048	0.0042	0.0016
	Percent eigenvalue (%)	89.0947	4.9383	4.3210	1.6461
2020	NDVI	0.6089	0.1932	0.5865	−0.4977
	LST	−0.3496	0.9141	−0.0931	−0.1826
	WET	0.4286	−0.0013	−0.8003	−0.4191
	NDBSI	−0.5684	−0.3563	0.0820	−0.7370
	Eigenvalue	0.0782	0.0054	0.0042	0.0015
	Percent eigenvalue (%)	87.5700	6.0470	4.7032	1.6797

Figure 3 reflects the interannual variation trend of the regional averages of each indicator. NDVI and WET showed a fluctuating upward trend, but NDBSI and LST followed the opposite trend. To be specific, the lowest and highest NDVI values occurred in 2000 (0.327) and 2020 (0.477), respectively, with an increase of 0.15. The lowest and highest LST values were in 2012 (27.126 °C) and 2000 (30.056 °C), respectively, with a change rate of 7.385% from 2000 to 2020. The WET mean for the LP varied for different years, and it increased by 7.170%. Meanwhile, the NDBSI had the largest change percentage, with a decrease of 95.778%. Moreover, RSEI showed a fluctuating upward trend from 0.396 to 0.522, which showed an increasing trend of 0.005 (year^{-1}). On the whole, the four indicators played a positive role on RSEI, which is consistent with the change trend of RSEI in the LP.

4.1.2. Spatiotemporal Changes of RSEI in the LP

In order to quantitatively analyze the ecological status in the LP, RSEI was divided into five classes at 0.2 intervals, representing poor (0–0.2), fair (0.2–0.4), moderate (0.4–0.6), good (0.6–0.8) and excellent (0.8–1) [52]. The environmental quality of the LP gradually improved from northwest to southeast (Figure 4), showing a spatial pattern of "excellent in the southeast and poor in the northwest".
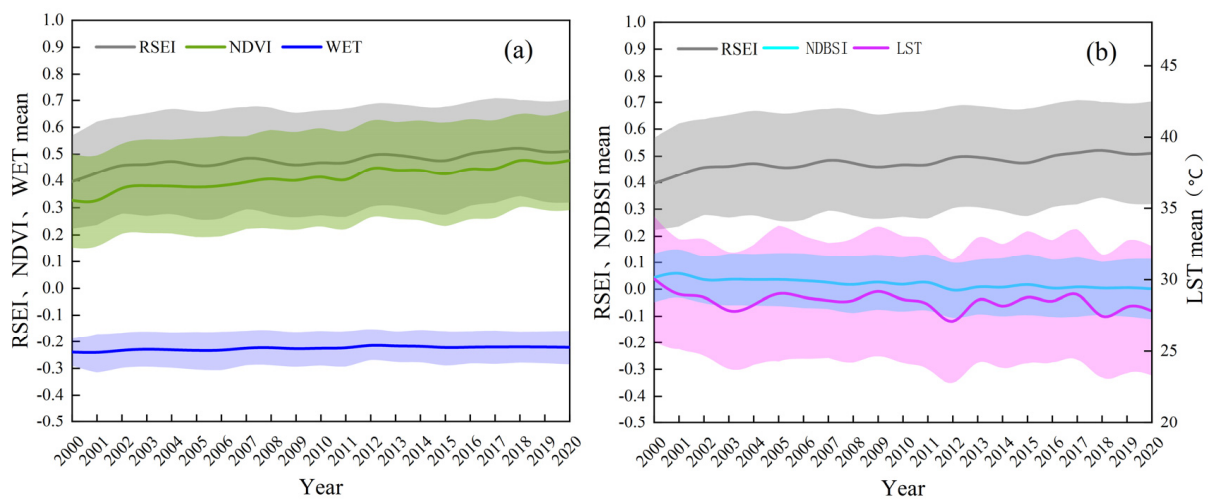
Figure 3. The interannual variation trend of each indicator. (**a**) the regional averages of RSEI, NDVI, WET indicators, and (**b**) the regional averages of RSEI, NDBSI, LST indicators.
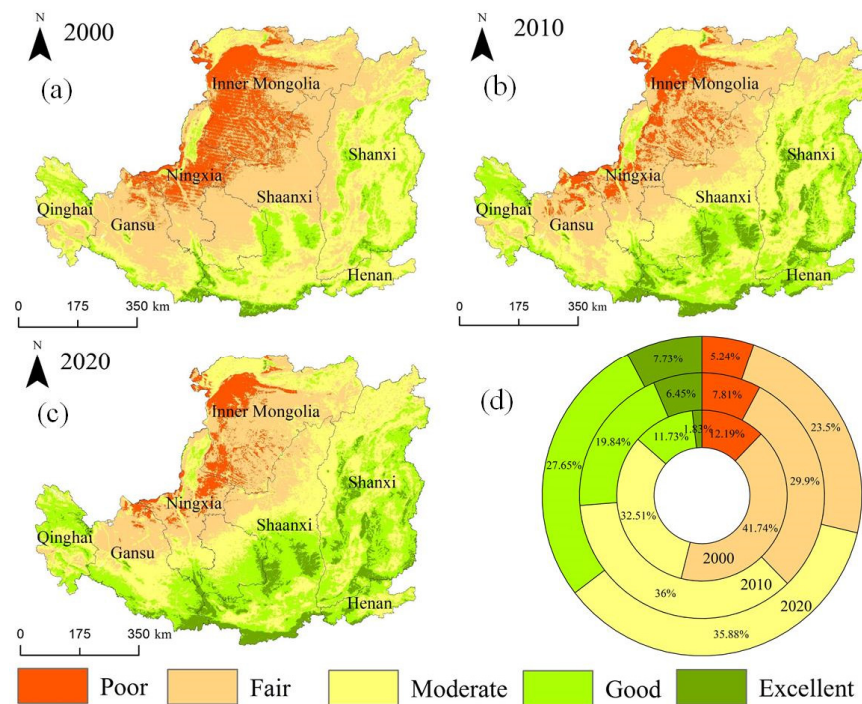

Figure 4. Spatiotemporal changes of RSEI in the Loess Plateau during 2000 (**a**), 2010 (**b**) and 2020 (**c**) and the ratio of each RSEI class from 2000–2020 (**d**).

In terms of the spatial distribution of RSEI, the areas with poor and fair levels, which were mainly distributed in the northwest, such as northern Inner Mongolia, Ningxia, Gansu, Shaanxi, decreased significantly. In contrast, the areas with good and excellent levels, which were located in the southeast of the study area, mostly around southern Henan, Shanxi and Shaanxi, increased significantly. This is mainly because the main vegetation types in the southeast are warm-temperate deciduous forest, while the northwest of the study area is mainly grassland and desert steppe, which have worse ecological self-regulation ability than the southeast LP.

In terms of the ratio of each RSEI class, the area with poor and fair ecological levels decreased by 160,800 km^2, while the area with good and excellent ecological levels increased by 139,100 km^2. In addition, the overall environmental quality was primarily at the fair level, with an area proportion of 41.74%. In 2010 and 2020, the RSEI was mainly at the

moderate level, accounting for 36.00% and 35.88% of the total area. The environmental quality reached the optimal level in 2020.

4.1.3. RSEI Transfer Analysis

Figures 5 and 6 reveal the changes of environmental quality at different levels in the LP from 2000 to 2020, when the proportion of the poor and fair levels decreased, while the good and excellent levels expanded. Among these, about 35,310 and 190 km^2 of poor levels was transformed into fair and moderate levels, respectively. In addition, 29,700 km^2 of good RSEI was converted to excellent level. From 2010 to 2020, the area of good and excellent levels continued to expand, while poor, fair and moderate levels decreased. Approximately 21,700 km^2 of poor level was converted to fair level, while fair level was mainly converted into moderate (58,500 km^2) and poor level (5600 km^2). During this period, the expansion of good level was mainly from moderate (68,000 km^2) and excellent level (2100 km^2). At the same time, some of the excellent levels were converted to moderate levels.
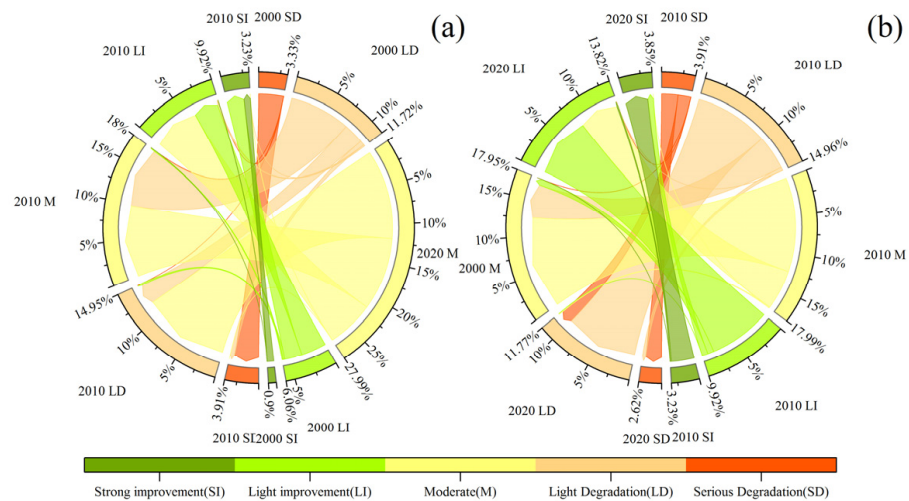

Figure 5. Sankey of RSEI transfer matrix from (**a**) 2000–2010 and (**b**) 2010–2020.
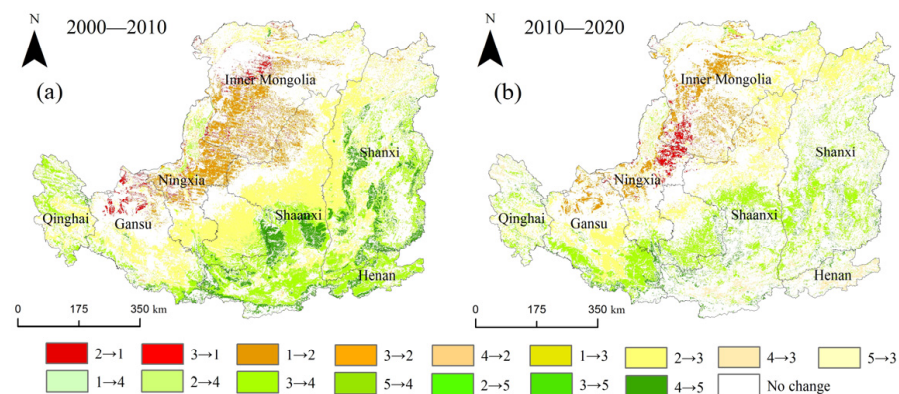

Figure 6. Spatial changes of RSEI in the Loess Plateau from (**a**) 2000–2010 and (**b**) 2010–2020. Note: 1: poor, 2: fair; 3: moderate; 4: good; 5: excellent.

By comparing the changes of RSEI transfer from 2000 to 2010 and from 2010 to 2020, the improved regions of RSEI were larger than the degraded regions. The improved areas were in the southeast of the study area, such as the south of Shaanxi and Henan, while the degraded areas were in the north of Gansu and the northwest of Ningxia. The no change area was mainly in the middle of the LP.

4.2. Trend Analysis of RSEI and Its Indicators in the LP

The Sen–Mann–Kendall method was used to detect the long-term change trend of RSEI. Figure 7a–d present the change trend of NDVI, LST, WET and NDBSI indicators. The improved area of NDVI and WET accounted for more than 90% and 60%, respectively, which was widely distributed in the LP. Both of them had a positive impact on RSEI. However, LST and NDBSI had a negative impact, accounting for more than 70% of the LP. The WET and NDVI with positive benefits remarkably increased, while the LST and NDBSI with negative benefits decreased significantly, leading to the promotion of RSEI, which was consistent with Figure 7e.
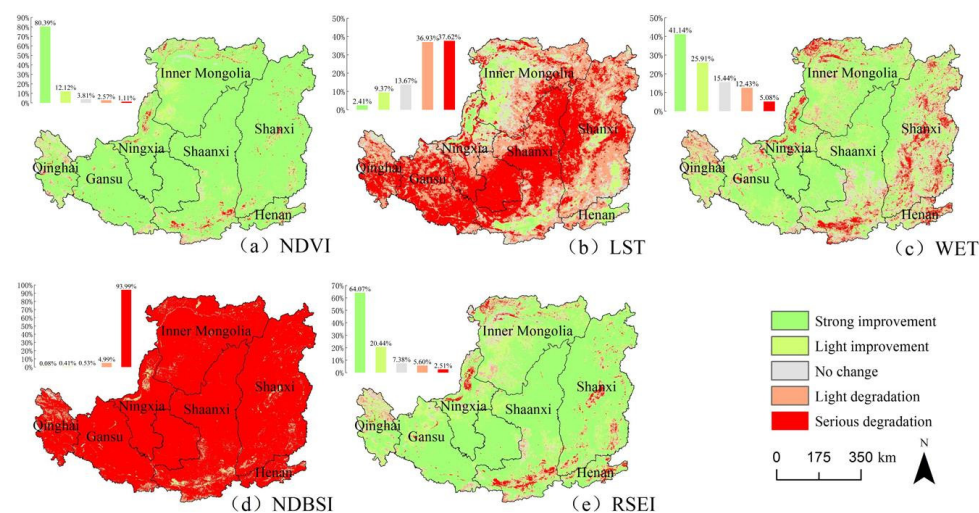

Figure 7. Changing trends of each indicator: (**a**) changing trends of NDVI; (**b**) changing trends of LST; (**c**) changing trends of WET; (**d**) changing trends of NDBSI; (**e**) changing trends of NDBSI.

Approximately 7.38% of the regional RSEI remained stable, mainly in northern Inner Mongolia, northern Ningxia and southern Shaanxi (Figure 7e). The majority (84.51%) of the regional environmental quality in the LP was improved. In other words, the areas with significant improvement were widely distributed in all counties, and slight improvements were mostly distributed in Inner Mongolia, northern Gansu, northern Ningxia and eastern Shanxi. The areas of degradation were very small, accounting for only 8.11%, which occurred in the north and southeast of the study area.

4.3. Relationship between Land Use Change and RSEI

Land use/land cover (LULC) changes are the most basic and prominent landscape features describing the impact of human disturbance on the earth surface [51]. Thus, the impact of LULC on RSEI was thoroughly analyzed by combing land use maps of the LP in the past 20 years (Figure 8). As can be seen from Figure 8 and Table 4, the region experienced dramatic land use changes during 2000–2020, with increases in forest, water and construction land, and a shrinking of farmland, grassland and unused land. The highest and lowest forest percentages were found in 2020 (16.90%) and 2000 (15.45%), and the increase rate from 2000 to 2010 (1.16%) was greater than that from 2010 to 2020 (0.29%), which had a positive effect on the RSEI. Construction land was mostly located in the southeastern part of the study area. However, the increase rate of construction land from 2010 to 2020 (1.77%) was higher than that from 2000 to 2010 (0.50%), which had a negative effect on the RSEI. The contribution of NDVI was higher than that of NDBSI in PC1 (Table 3), suggesting that the improvement rate of RSEI from 2000 to 2010 was higher than that from 2010 to 2020. Both farmland and grassland areas decreased and mainly turned into forest and construction land (Figure 8). The overall changes of unused land and waters were not obvious, which was consistent with previous studies [37,53,54].
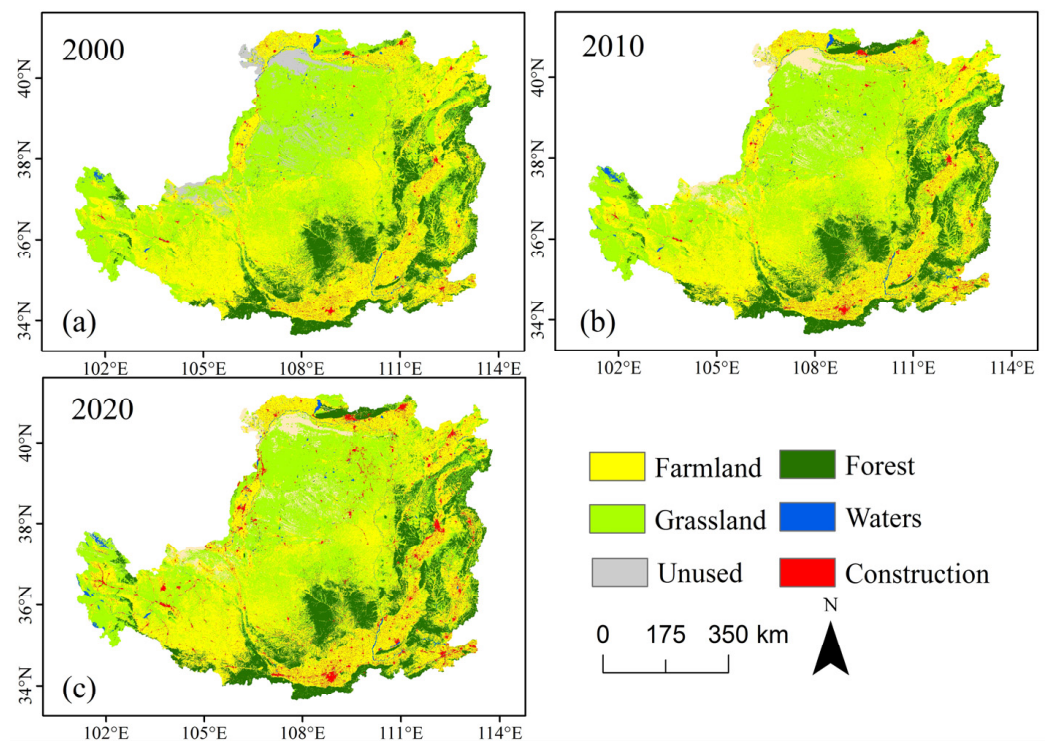
Figure 8. Spatiotemporal distribution of land use types of (**a**) 2000, (**b**) 2010 and (**c**) 2020 in the Loess Plateau.

Table 4. Statistical results of different land types in the LP (2000–2020).

Land Use Types	Proportion of the Corresponding Area		
	2000	**2010**	**2020**
Farmland	40.02%	39.33%	38.95%
Forest	15.45%	16.61%	16.90%
Grassland	38.04%	37.04%	35.45%
Waters	0.69%	0.76%	0.91%
Unused	3.93%	3.89%	3.65%
Construction	1.87%	2.37%	4.14%

Figure 9 presents the RSEI mean values of different land use types. The mean RSEI differed by land-use classes; moreover, the RSEI of all land-use types have improved on the whole, indicating a trend of continuous environmental improvement in the past 20 years in this region. Past studies have shown that vegetation can effectively reduce soil erosivity and help increase the resistance and carrying capacity of the environment [5]. Therefore, forest areas provide favorable ecological conditions. As can be seen from Table 3, NDBSI had a negative effect on RSEI, indicating that construction and unused land contributed to lowering the environmental quality. In summary, while vegetation is closely related to the overall environmental quality, human activities accelerate the transformation and change of LULC and ultimately degrade environmental quality. Therefore, to improve the environment in the future, continuous forest restoration is essential, and land consolidation should be strengthened to optimize the balance between urban construction and sustainable development.
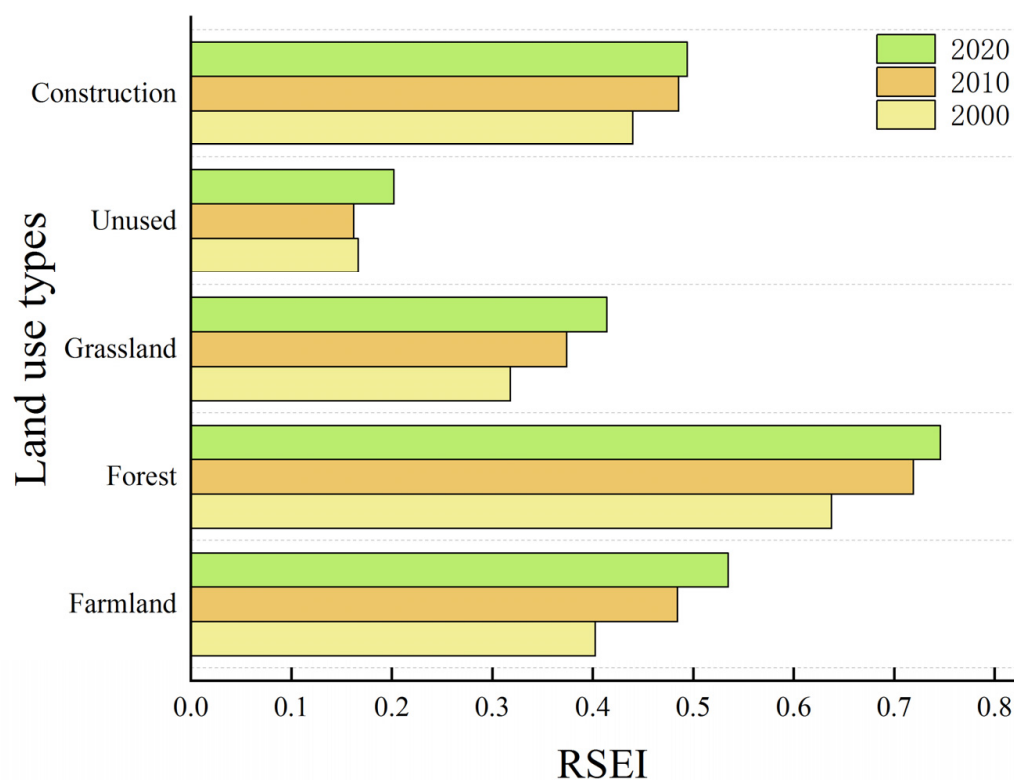
Figure 9. Mean RSEI of each land use types.

4.4. Analysis of Driving Mechanism of RSEI

4.4.1. Single-Factor Detection Results

Model factors (NDVI, LST, WET and NDBSI) are closely related to natural factors such as rainfall and temperature; therefore, rainfall and temperature were not considered among the natural factors. Table 5 shows the factor detection results of the geographical detector model. The *p* values of all factors in the LP in 2000, 2010 and 2020 were all 0, indicating that the selected factors had a significant impact on the spatial distribution of RSEI in the LP. In terms of model factors, the explanatory power of NDVI and NDBSI on RSEI was higher than Wet and LST. In 2000, the order of the influence degree of socio-economic and natural factors on RSEI was as follows: X4 (0.2447) > X6 (0.1718) > X3 (0.1284) > X2 (0.0947) > X1 (0.0946) > X5 (0.0880). Land use types had the greatest impact on RSEI, followed by slope, indicating that natural factors had a more significant impact on RSEI than socioeconomic factors. However, in this period, economic development was slow, and agriculture and husbandry were the main economic source; thus, the explanatory power of X3 was higher than X2. In 2010, the land use types factor was still the main factor driving RSEI, and GDP was the second most influencing factor, which indicated that the influence of GDP significantly increased, with a value of 0.265. In 2020, the order of explanatory power was as follows: X2 (0.3161) > X4 (0.2937) > X6 (0.2420) > X3 (0.1366) > X5 (0.0642) > X1 (0.0175). At this time, GDP had the greatest explanatory power on RSEI, followed by land use types, indicating that with rapid socioeconomic development, the driving force of social factors strengthened and became a key factor affecting the RSEI. It was found that population density and elevation had the least effect on RSEI, while other factors had varying effects on RSEI in the study area.

Table 5. Influence of factors on RSEI between 2000 and 2020.

Year		Socioeconomic Factors			Natural Factors			Model Factors		
	Factors	X1	X2	X3	X4	X5	X6	X7	X8	X9	X10
2000	q	0.0108	0.0947	0.1284	0.2447	0.0880	0.1718	0.7990	0.6366	0.7288	0.7987
	p	0.000	0.000	0.000	0.000	0.000	0.000	0.000	0.000	0.000	0.000
2010	q	0.0150	0.2654	0.1288	0.2855	0.0807	0.2011	0.8188	0.6559	0.7637	0.8477
	p	0.000	0.000	0.000	0.000	0.000	0.000	0.000	0.000	0.000	0.000
2020	q	0.0175	0.3161	0.1366	0.2937	0.0642	0.2420	0.8279	0.6356	0.7596	0.8357
	p	0.000	0.000	0.000	0.000	0.000	0.000	0.000	0.000	0.000	0.000

4.4.2. Multi-Factor Detection Results

The interaction results of ten factors are shown in Figure 10. There was a significant double synergistic or nonlinear enhancement effect between all the factors, indicating that the interaction of any two factors can enhance the explanatory power of the spatial differentiation of RSEI than one factor. In 2000, the interaction of NDVI and WET was the greatest, with a q value of 0.88. In 2010 and 2020, the interaction between NDVI and NDBSI reached 0.89 and 0.90, respectively. The interactions between NDBSI and slope, and between land-use types and elevation were relatively strong. Model factors and natural factors were found to be decisive factors affecting RSEI, as they could strongly explain the differentiation of RSEI. Additionally, for population density and elevation with a weak explanatory power of a single factor, the explanatory power was significantly enhanced after acting together with other influencing factors. For example, in 2020, the maximum explanatory power of population density and elevation was 0.06, while the interaction influence with other factors was between 0.16 and 0.86. This shows that the RSEI in the LP was the combined result of multiple factors.
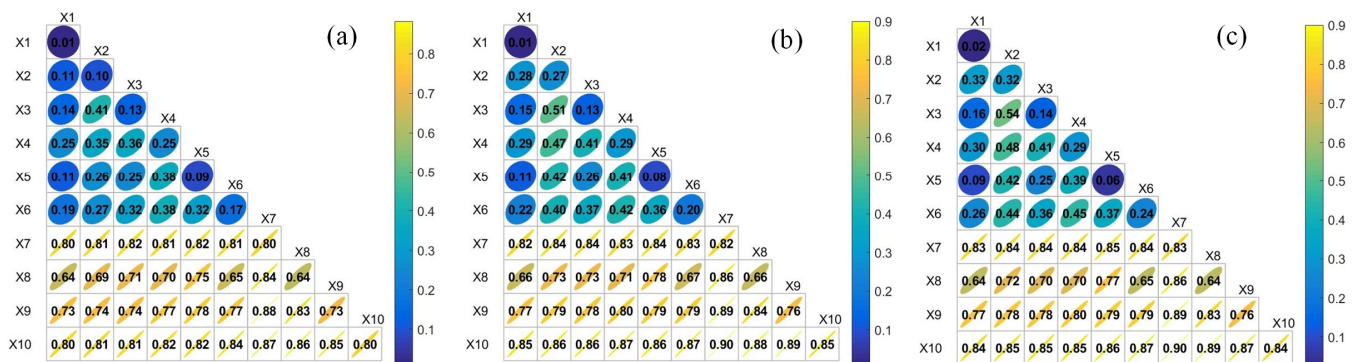

Figure 10. Interaction detection in (**a**) 2000, (**b**)2010 and (**c**) 2020 of impact factors.

4.4.3. Optimal Ranges and Tipping Points of Factors Influencing RSEI

Mean RSEI had minima and maxima of 0.45 and 0.58, respectively, when X1 ranged from 0–57.9 and 373–737 people/km² (Figure 11a). Furthermore, lower X2 (2790–3970 hundred million yuan), X3 (222–287 hundred million yuan), X4 (80–90), X5 (1310–1420 m), and X6 (0.66–1.42) ranges resulted in lower NDVI values (0.31, 0.37, 0.2, 0.42, and 0.38, respectively;) (Figure 11b–f). In addition, X7 and X9 showed that RSEI increased (0.84 and 0.78) with an increase in greenness and wetness (Figure 11g,i). Finally, X8 (0.75–0.99) and X10 (0.72–0.84) ranges indicated that RSEI decreased with an increase in heat and dryness (Figure 11h,j).
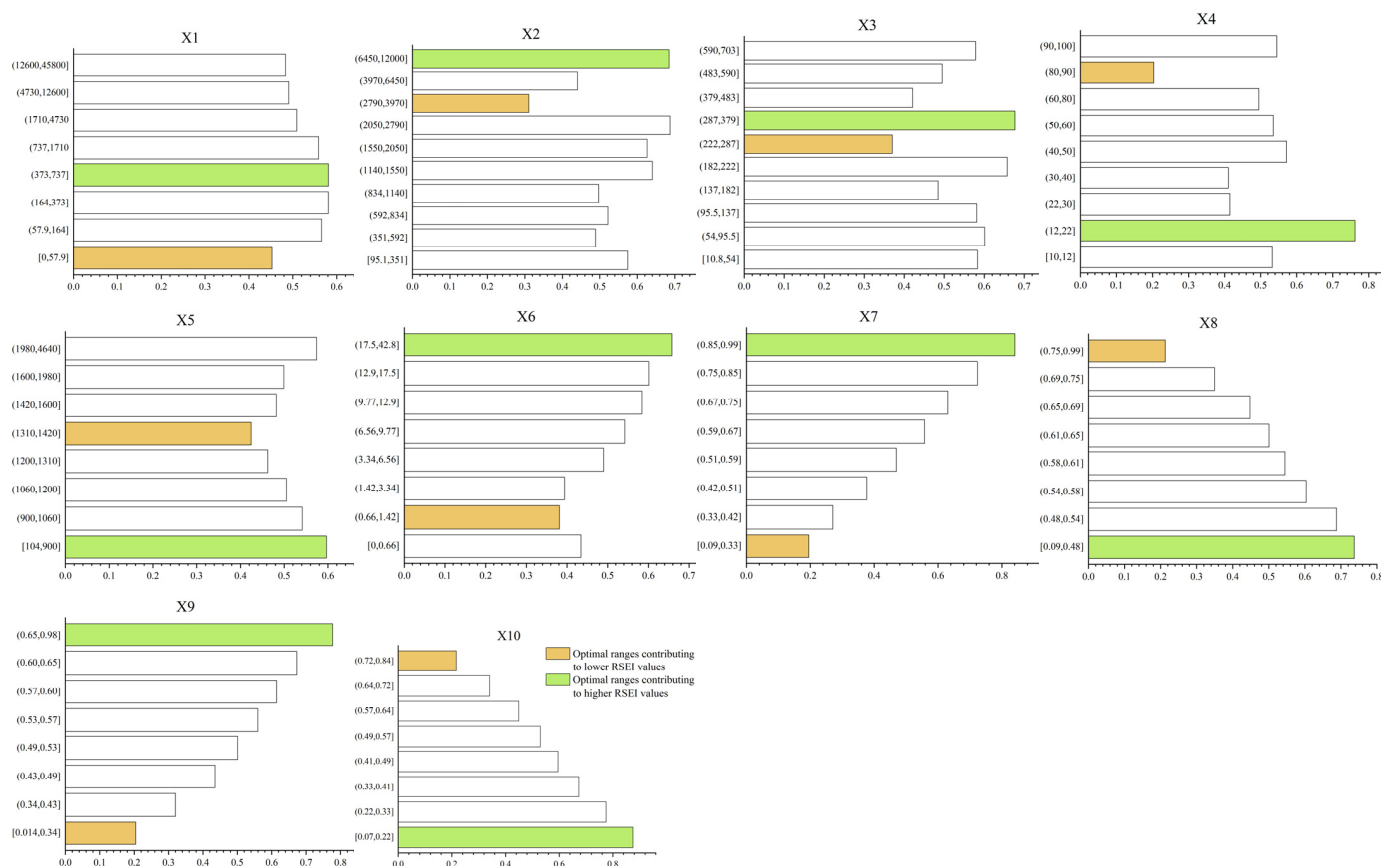
Figure 11. Optimal ranges and tipping points of drivers influencing RSEI. Note: X1–X10 same as in Table 2.

5. Discussion

5.1. Process of Ecological Restoration in the LP

In order to deeply understand the impact of economic development and environmental protection policies on RSEI, A, B, C and D in Figure 1 were analyzed. Figure 12 shows the RSEI distribution and RSEI variation curves in the four regions during the past 20 years.

The significant improvement of RSEI of A and B is inseparable from the implementation of regional policies in the LP. Environmental management in the LP can be divided into the following stages: (1) From the 1950s to the 1970s, the mode of slope management, with the joint management of gullies and slopes, was initiated. Afforestation, terraced fields and large-scale dams were implemented to control soil erosion, increase grain production and intercept sediment. (2) From the 1980s to the 1990s, comprehensive management of small watersheds and three-north shelterbelt construction were carried out [55,56]. A comprehensive soil and water loss control system was formed by actualizing a series of projects, such as constructing a shelterbelt system, constantly optimizing farmland structure, and implementing soil and water conservation measures such as furrow and ridge cultivation and contour cultivation. (3) Since 2000, farmland to forest and grassland conversion, slope farmland renovation and land building from ditches were implemented to reduce soil erosion on degraded farmland and steep slopes through forest or grassland covering and saline land reformation [57]. (4) In 2016, the Shaanxi region of the LP was listed as one of the first national pilot projects for environmental protection aiming to coordinate land consolidation and at remediation of soil pollution, water protection and regional ecosystem comprehensive management. (5) At the end of 2018, the Ministry of Water Resources of People's Republic of China approved the Comprehensive Management Plan for Fixing Ditches and Preserving Tableland in the LP Gully Region (2015–2025). The plan aims to control the watershed area of 2829.77 km^2, protect the plateau area of 1348.23 km^2 and treat 8968 eroded ditches. Since the implementation of the above series of policies, the forest

coverage rate in the study area has increased by 12% to 31.9% [58]. At the same time, the afforestation protection area of Mu Us sandy land has reached to 2.24 million hectares due to the implementation of the three-north shelterbelt project [5]. This effectively prevented the expansion of sand and was conducive to the improvement of ecosystem function [59]. By 2015, soil protection measures such as contour tillage, barrage, plastic film mulching and straw mulching were fulfilled to prevent and control soil erosion [60]. As a result, the sediment transported from the LP to the middle reaches of the Yellow River dropped sharply from 1.6 billion tons to 140 million tons [47] and average soil erosion decreased from 47.37 to 18.77 t/hm^2 [58], reducing ecological vulnerability. Figure 1A (right) also confirms the ecological benefits brought by the above policies, showing that a large amount of cultivated land was converted to vegetation.
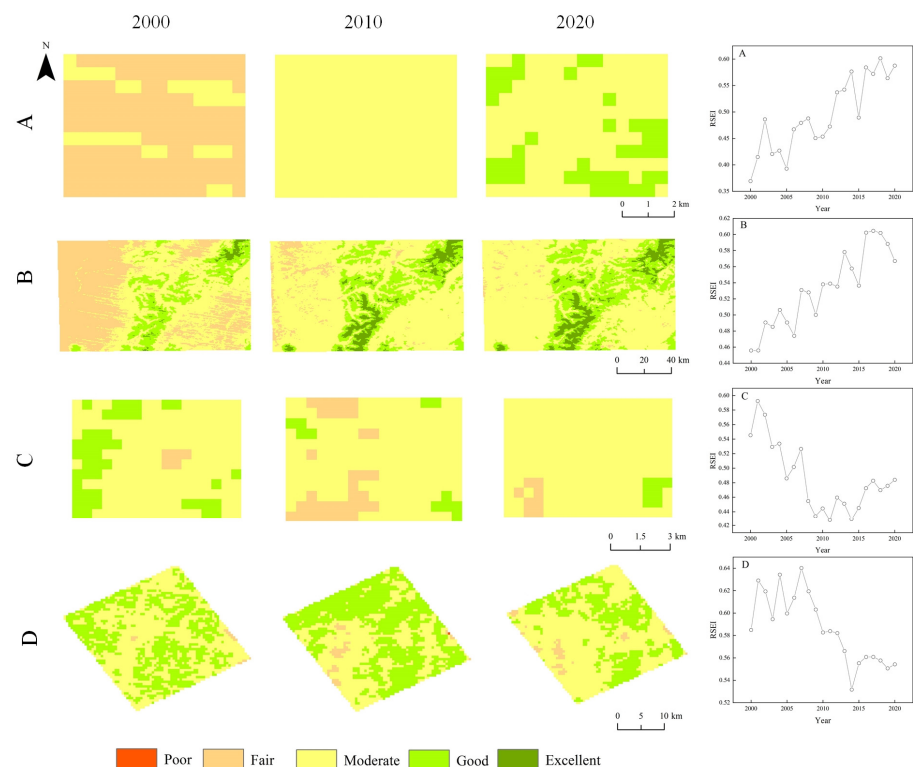
Figure 12. Spatiotemporal changes and curve of RSEI in A, B, C and D from 2000 to 2020.

The RSEI of Figure 1C,D shows a trend of decline due to the concentration of population and high urbanization in these regions. In addition, the implementation of the National New Urbanization Plan (China Central Government portal, 2014) has accelerated the economic development level of most cities in the LP [36]. Combined with Figure 1D, it can be seen that economic improvement was accompanied by urban expansion, which had a negative impact on RSEI.

5.2. Major Drivers of RSEI

RSEI change is a complex process affected by both natural and anthropogenic factors, which is consistent with the conclusion of past reports [49]. Our results showed that model factors explained most changes of RSEI in the LP, followed by natural factors such as land use types and slope. As for socioeconomic factors, the explanatory power of GDP gradually increased on the RSEI. Su et al. [53] reached a similar conclusion when studying the effects of climate change and land-use change in the LP. The GDP and per capita GDP continued to grow during this period, with annual growth rates of 15.23% and 14.30% [5]. Excessive economic development and population growth were accompanied by increased demand for construction land, which occupied nearby farmland, expanded the scope of industrial activities, and increased disturbance increasing environmental pressure [61]. Therefore,

this phenomenon is an important reason for the continuous enhancement of their influence on RSEI in the later period (Table 5). In the early period, owing to the underdeveloped economy, most of farmers' income came from agricultural production activities. Although the arable land area was decreasing (Table 4), the progress of farming methods and the improvement of agricultural machinery promoted agricultural income in the later period. In addition, the planting of high-quality grasslands reduced the negative impact of a grazing ban on animal husbandry. Therefore, the gross output values of agriculture, forestry, animal husbandry and fishery also explain most of the variation in RSEI.

Our results showed that land use change was an important factor affecting RSEI, and vegetation was the main land use mode in the LP, accounting for more than 54% of the area. Furthermore, as an important component of the ecosystem, vegetation is connected with the atmosphere, water and carbon cycle and other natural processes; thus, it has an important impact on monitoring the changes of the ecosystem [62]. In addition, Mehri et al. [63] reported that vegetation played an important role in soil texture. Moreover, wetness promotes climate regulation and the water cycle of land, and affects evaporation and vegetation growth collaborating with LST [2,64]. Therefore, it has become the primary influencing factor on RSEI. At the same time, slope was also the main driving factor, partly because a steeper slope accelerates the runoff of a large amount of sediment and organic matter, resulting in lower erosion resistance [65].

5.3. Limitations and Future Work

Only four indicators were considered in the present study, and the impact of the economy and air pollution on the environment were ignored. In addition, low resolution MODIS data used in this paper prevent a detailed expression of the characteristics of environmental quality. High-resolution images and new indicators will be introduced in our subsequent research to comprehensively and elaborately evaluate the environmental quality in this region. Considering that the driving factors of RSEI were analyzed by county and district, and the economic conditions of each county and district are different, future research will fully consider the regional differences and further analyze and explore the socioeconomic influencing factors of ecological quality. Additionally, in the future, we will forecast environmental quality based on functional regression models [66].

6. Conclusions

Based on the GEE platform and MODIS data, environmental quality in the LP from 2000 to 2020 was comprehensively evaluated, and a geographical model was used to explore driving forces of environmental quality from three aspects involving socioeconomic factors, natural factors and model factors. The results showed that: Firstly, the contribution rates of PC1 were more than 86%, demonstrating that RSEI could be applicable on a large scale. In addition, average RSEI values for 2000, 2010 and 2020 were 0.396, 0.468 and 0.511, respectively, showing an overall upward trend with a growth rate of 29.04%, which indicated that over the past 20 years, the environmental quality in the LP significantly improved. Secondly, in the past 20 years, the areas with poor and fair RSEI levels continued to decrease (160,800 km^2), mainly in the northern region of the LP, including Inner Mongolia and Ningxia. At the same time, areas with good and excellent RSEI levels significantly increased (139,100 km^2) in the southern LP, such as in Henan, Shanxi and southern Shaanxi. Thirdly, from 2000 to 2020, 84.51% of the RSEI in the LP improved in all counties and districts. The degraded regions (8.11%) were mainly located in the north and southeast of the LP. The stable regions were mostly distributed in vast areas of northern Inner Mongolia, northern Ningxia and southern Shaanxi. Finally, single factor detection analysis showed that model and natural factors were the leading factors influencing the spatial–temporal distribution of RSEI. Among socioeconomic factors, GDP had an increasing explanatory power. The contribution of multi-factor interaction was stronger than that of a single factor. The explanatory powers of model factors were relatively stronger. Furthermore, the study results provided optimal ranges and tipping points of drivers that RSEI dynamics in the LP.

References

1. Ji, J.; Wang, S.; Zhou, Y.; Liu, W.; Wang, L. Spatiotemporal Change and Landscape Pattern Variation of Eco-Environmental Quality in Jing-Jin-Ji Urban Agglomeration From 2001 to 2015. *IEEE Access* **2020**, *8*, 125534–125548. [CrossRef]
2. Ji, J.; Tang, Z.; Zhang, W.; Liu, W.; Jin, B.; Xi, X.; Wang, F.; Zhang, R.; Guo, B.; Xu, Z.; et al. Spatiotemporal and Multiscale Analysis of the Coupling Coordination Degree between Economic Development Equality and Eco-Environmental Quality in China from 2001 to 2020. *Remote Sens.* **2022**, *14*, 737. [CrossRef]
3. Xu, H.; Wang, Y.; Guan, H.; Shi, T.; Hu, X. Detecting Ecological Changes with a Remote Sensing Based Ecological Index (RSEI) Produced Time Series and Change Vector Analysis. *Remote Sens.* **2019**, *11*, 2345. [CrossRef]
4. An, M.; Xie, P.; He, W.; Wang, B.; Huang, J.; Khanal, R. Spatiotemporal change of ecologic environment quality and human interaction factors in three gorges ecologic economic corridor, based on RSEI. *Ecol. Indic.* **2022**, *141*, 109090. [CrossRef]
5. Yurui, L.; Xuanchang, Z.; Zhi, C.; Zhengjia, L.; Zhi, L.; Yansui, L. Towards the progress of ecological restoration and economic development in China's Loess Plateau and strategy for more sustainable development. *Sci. Total Environ.* **2021**, *756*, 143676. [CrossRef] [PubMed]
6. Uchida, E.; Xu, J.; Rozelle, S. Grain for Green: Cost-Effectiveness and Sustainability of China's Conservation Set-Aside Program. *Land. Econ.* **2005**, *81*, 247–264. [CrossRef]
7. Chen, H.; Fleskens, L.; Schild, J.; Moolenaar, S.; Wang, F.; Ritsema, C. Impacts of large-scale landscape restoration on spatio-temporal dynamics of ecosystem services in the Chinese Loess Plateau. *Landsc. Ecol.* **2022**, *37*, 329–346. [CrossRef]
8. Su, K.; Liu, H.; Wang, H. Spatial-Temporal Changes and Driving Force Analysis of Ecosystems in the Loess Plateau Ecological Screen. *Forests* **2022**, *13*, 54. [CrossRef]
9. Frazier, A.E.; Bryan, B.A.; Buyantuev, A.; Chen, L.; Echeverria, C.; Jia, P.; Liu, L.; Li, Q.; Ouyang, Z.; Wu, J.; et al. Ecological civilization: Perspectives from landscape ecology and landscape sustainability science. *Landsc. Ecol.* **2019**, *34*, 1–8. [CrossRef]
10. Wu, Z.; Dai, X.; Li, B.; Hou, Y. Livelihood consequences of the Grain for Green Programme across regional and household scales: A case study in the Loess Plateau. *Land Use Policy* **2021**, *111*, 105746. [CrossRef]
11. Wang, S.; Peng, J.; Zhuang, J.; Kang, C.; Jia, Z. Underlying mechanisms of the geohazards of macro Loess discontinuities on the Chinese Loess Plateau. *Eng. Geol.* **2019**, *263*, 105357. [CrossRef]
12. Li, P.; Chen, J.; Zhao, G.; Holden, J.; Liu, B.; Chan, F.K.S.; Hu, J.; Wu, P.; Mu, X. Determining the drivers and rates of soil erosion on the Loess Plateau since 1901. *Sci. Total Environ.* **2022**, *823*, 153674. [CrossRef] [PubMed]

13. Jiang, H.; Fan, G.; Zhang, D.; Fan, Y. Evaluation of Eco-environmental Quality of Coal Mining Area Using Multi-source Data. *Sci. Rep.* **2022**, *12*, 6623. [CrossRef]

14. Kasischke, E.S.; French, N.H.F.; Harrell, P.; Christensen, N.L.; Ustin, S.L.; Barry, D. Monitoring of wildfires in Boreal Forests using large area AVHRR NDVI composite image data. *Sci. Total Environ.* **1993**, *45*, 61–71. [CrossRef]

15. Nagler, P.L.; Scott, R.L.; Westenburg, C.; Cleverly, J.R.; Glenn, E.P.; Huete, A.R. Evapotranspiration on western U.S. rivers estimated using the Enhanced Vegetation Index from MODIS and data from eddy covariance and Bowen ratio flux towers. *Remote Sens. Environ.* **2005**, *97*, 337–351. [CrossRef]

16. Dousset, B.; Gourmelon, F. Satellite multi-sensor data analysis of urban surface temperatures and landcover. *ISPRS J. Photogramm. Remote Sens.* **2003**, *58*, 43–54. [CrossRef]

17. Zheng, Z.; Wu, Z.; Chen, Y.; Guo, C.; Marinello, F. Instability of remote sensing based ecological index (RSEI) and its improvement for time series analysis. *Sci. Total Environ.* **2022**, *814*, 152595. [CrossRef]

18. Becker, F.; Choudhury, B.J. Relative sensitivity of normalized difference vegetation Index (NDVI) and microwave polarization difference Index (MPDI) for vegetation and desertification monitoring. *Remote Sens. Environ.* **1988**, *24*, 297–311. [CrossRef]

19. Khan, J.; Wang, P.; Xie, Y.; Wang, L.; Li, L. Mapping MODIS LST NDVI Imagery for Drought Monitoring in Punjab Pakistan. *IEEE Access* **2018**, *6*, 19898–19911. [CrossRef]

20. Chang, Y.; Hou, K.; Wu, Y.; Li, X.; Zhang, J. A conceptual framework for establishing the index system of ecological environment evaluation-A case study of the upper Hanjiang River, China. *Ecol. Indic.* **2019**, *107*, 105568. [CrossRef]

21. Xu, H. A remote sensing urban ecological index and its application. *Acta Ecol. Sin.* **2013**, *33*, 7853–7862. (In Chinese)

22. Zou, Z.-h.; Yun, Y.; Sun, J.-n. Entropy method for determination of weight of evaluating indicators in fuzzy synthetic evaluation for water quality assessment. *J. Environ.* **2006**, *18*, 1020–1023. [CrossRef]

23. Saaty, T.L. A scaling method for priorities in hierarchical structures. *J. Math. Psychol.* **1977**, *15*, 234–281. [CrossRef]

24. Liu, B.; Zhang, F.; Wan, W.; Luo, X. Multi-objective Decision-Making for the Ecological Operation of Built Reservoirs Based on the Improved Comprehensive Fuzzy Evaluation Method. *Water Resour. Manag.* **2019**, *33*, 3949–3964. [CrossRef]

25. Dinh, T.C.; Dinh, T.C.; Anh, T.T.; Xuan, B.M.; Manh, L.N.; Van Thanh, D.; Le Van, D.; Thanh, H.D.; Quang, T.N. Mapping Seismic Zones Based on the Geomorphic Indices and the Analytic Hierarchy Process (AHP): A Case Study in Cao Bang Province and Adjacent Areas (Vietnam). *J. Geol. Soc. India* **2021**, *97*, 1565–1573. [CrossRef]

26. Maity, S.; Das, S.; Pattanayak, J.M.; Bera, B.; Shit, P.K. Assessment of ecological environment quality in Kolkata urban agglomeration, India. *Urban Ecosyst.* **2022**, *25*, 1137–1154. [CrossRef]

27. Qureshi, S.; Alavipanah, S.K.; Konyushkova, M.; Mijani, N.; Fathololomi, S.; Firozjaei, M.K.; Homaee, M.; Hamzeh, S.; Kakroodi, A.A. A Remotely Sensed Assessment of Surface Ecological Change over the Gomishan Wetland, Iran. *Remote Sens.* **2020**, *12*, 2898. [CrossRef]

28. Gorelick, N.; Hancher, M.; Dixon, M.; Ilyushchenko, S.; Thau, D.; Moore, R. Google Earth Engine: Planetary-scale geospatial analysis for everyone. *Remote Sens. Environ.* **2017**, *202*, 18–27. [CrossRef]

29. Yang, X.; Meng, F.; Fu, P.; Zhang, Y.; Liu, Y. Spatiotemporal change and driving factors of the Eco-Environment quality in the Yangtze River Basin from 2001 to 2019. *Ecol. Indic.* **2021**, *131*, 108214. [CrossRef]

30. Sen, P.K. Estimates of the Regression Coefficient Based on Kendall's Tau. *J. Am. Stat. Assoc.* **1968**, *63*, 1379–1389. [CrossRef]

31. Kendall, M.G. *Rank Correlation Methods*; Springer: Boston, MA, USA, 1948.

32. Mann, H.B. Nonparametric Tests Against Trend. *Econometrica* **1945**, *13*, 245. [CrossRef]

33. Yin, S. Decadal trends of MERRA-estimated PM2.5 concentrations in East Asia and potential exposure from 1990 to 2019. *Atmos. Environ.* **2021**, *264*, 118690. [CrossRef]

34. Ruiz-Alvarez, O.; Singh, V.P.; Enciso-Medina, J.; Ontiveros-Capurata, R.E.; Corrales-Suastegui, A. Spatio-Temporal Trends of Monthly and Annual Precipitation in Aguascalientes, Mexico. *Atmosphere* **2020**, *11*, 437. [CrossRef]

35. Lü, Y.; Fu, B.; Feng, X.; Zeng, Y.; Liu, Y.; Chang, R.; Sun, G.; Wu, B. A policy-driven large scale ecological restoration: Quantifying ecosystem services changes in the Loess Plateau of China. *PLoS ONE* **2012**, *7*, e31782. [CrossRef]

36. Xiao, Y.; Wang, R.; Wang, F.; Huang, H.; Wang, J. Investigation on spatial and temporal variation of coupling coordination between socioeconomic and ecological environment: A case study of the Loess Plateau, China. *Ecol. Indic.* **2022**, *136*, 108667. [CrossRef]

37. Song, Y.; Xue, D.; Dai, L.; Wang, P.; Huang, X.; Xia, S. Land cover change and eco-environmental quality response of different geomorphic units on the Chinese Loess Plateau. *J. Arid Land* **2020**, *12*, 29–43. [CrossRef]

38. Huete, A.; Didan, K.; Miura, T.; Rodriguez, E.P.; Gao, X.; Ferreira, L.G. Overview of the radiometric and biophysical performance of the MODIS vegetation indices. *Remote Sens. Environ.* **2002**, *83*, 195–213. [CrossRef]

39. Airiken, M.; Zhang, F.; Chan, N.W.; Kung, H.T. Assessment of spatial and temporal ecological environment quality under land use change of urban agglomeration in the North Slope of Tianshan, China. *Environ. Sci. Pollut. Res. Int.* **2022**, *29*, 12282–12299. [CrossRef]

40. Lobser, S.; Cohen, W. MODIS tasselled cap: Land cover characteristics expressed through transformed MODIS data. *Int. J. Remote Sens.* **2007**, *28*, 5079–5101. [CrossRef]

41. Zhang, X.Y.; Schaaf, C.B.; Friedl, M.A.; Strahler, A.H.; Gao, F.; Hodges, J.C.F. MODIS tasseled cap transformation and its utility. In Proceedings of the IEEE International Geoscience and Remote Sensing Symposium, Toronto, ON, Canada, 24–28 June 2002; IEEE: Piscataway, NJ, USA, 2002; Volume 2, pp. 1063–1065.

42. Xu, H. A new index for delineating built-up land features in satellite imagery. *Int. J. Remote Sens.* **2008**, *29*, 4269–4276. [CrossRef]

43. Rikimaru, A.; Roy, P.S.; Miyatake, S. Tropical forest cover density mapping. *Trop Ecol.* **2002**, *43*, 39–47.

44. Wang, J.; Xu, C. Geodetector: Principle and prospective. *Acta Geogr. Sin.* **2017**, *72*, 116–134.

45. Li, Y.; Zhang, G.; Lin, T.; Ye, H.; Liu, Y.; Chen, T.; Liu, W. The spatiotemporal changes of remote sensing ecological index in towns and the influencing factors: A case study of Jizhou District, Tianjin. *Acta Ecol. Sin.* **2022**, *42*, 474–486.

46. Zhang, Q.-J.; Fu, B.-J.; Chen, L.-D.; Zhao, W.-W.; Yang, Q.-K.; Liu, G.-B.; Gulinck, H. Dynamics and driving factors of agricultural landscape in the semiarid hilly area of the Loess Plateau, China. *Agric. Ecosyst. Environ.* **2004**, *103*, 535–543. [CrossRef]

47. Sun, W.; Song, X.; Mu, X.; Gao, P.; Wang, F.; Zhao, G. Spatiotemporal vegetation cover variations associated with climate change and ecological restoration in the Loess Plateau. *Agric. For. Meteorol.* **2015**, *209–210*, 87–99. [CrossRef]

48. Naeem, S.; Zhang, Y.; Zhang, X.; Tian, J.; Abbas, S.; Luo, L.; Meresa, H.K. Both climate and socioeconomic drivers contribute to vegetation greening of the Loess Plateau. *Sci. Bull.* **2021**, *66*, 1160–1163. [CrossRef]

49. Yuan, B.; Fu, L.; Zou, Y.; Zhang, S.; Chen, X.; Li, F.; Deng, Z.; Xie, Y. Spatiotemporal change detection of ecological quality and the associated affecting factors in Dongting Lake Basin, based on RSEI. *J. Clean. Prod.* **2021**, *302*, 126995. [CrossRef]

50. Xia, Q.-Q.; Chen, Y.-N.; Zhang, X.-Q.; Ding, J.-L. Spatiotemporal Changes in Ecological Quality and Its Associated Driving Factors in Central Asia. *Remote Sens.* **2022**, *14*, 3500. [CrossRef]

51. Liu, C.; Li, W.; Zhu, G.; Zhou, H.; Yan, H.; Xue, P. Land Use/Land Cover Changes and Their Driving Factors in the Northeastern Tibetan Plateau Based on Geographical Detectors and Google Earth Engine: A Case Study in Gannan Prefecture. *Remote Sens.* **2020**, *12*, 3139. [CrossRef]

52. Ariken, M.; Zhang, F.; Liu, K.; Fang, C.; Kung, H.-T. Coupling coordination analysis of urbanization and eco-environment in Yanqi Basin based on multi-source remote sensing data. *Ecol. Indic.* **2020**, *114*, 106331. [CrossRef]

53. Su, C.; Fu, B. Evolution of ecosystem services in the Chinese Loess Plateau under climatic and land use changes. *Glob. Planet Chang.* **2013**, *101*, 119–128. [CrossRef]

54. Ren, Y.; Lü, Y.; Fu, B.; Comber, A.; Li, T.; Hu, J. Driving Factors of Land Change in China's Loess Plateau: Quantification Using Geographically Weighted Regression and Management Implications. *Remote Sens.* **2020**, *12*, 453. [CrossRef]

55. Liu, G. Soil Conservation and Sustainable Agriculture on the Loess Plateau: Challenges and Prospects. *Ambio* **1999**, *28*, 663–668.

56. Deng, X.-P.; Shan, L.; Zhang, H.; Turner, N.C. Improving agricultural water use efficiency in arid and semiarid areas of China. *Agric. Water Manag.* **2006**, *80*, 23–40. [CrossRef]

57. Bullock, A.; King, B. Evaluating China's Slope Land Conversion Program as sustainable management in Tianquan and Wuqi Counties. *J. Environ. Manag.* **2011**, *92*, 1916–1922. [CrossRef]

58. Li, Z.; Yang, L.; Wang, G.; Hou, J.; Xin, Z.; Liu, G.; Fu, B. The management of soil and water conservation in the Loess Plateau of China: Present situations, problems, and counter-solutions. *Acta Ecol. Sin.* **2019**, *39*, 7398–7409.

59. Du, X.; Zhao, X.; Liang, S.; Zhao, J.; Xu, P.; Wu, D. Quantitatively Assessing and Attributing Land Use and Land Cover Changes on China's Loess Plateau. *Remote Sens.* **2020**, *12*, 353. [CrossRef]

60. Ping, Z.; Anbang, W.; Xinbao, Z.; Xiubin, H. Soil conservation and sustainable eco-environment in the Loess Plateau of China. *Environ. Earth Sci.* **2013**, *68*, 633–639. [CrossRef]

61. Venkatesh, K.; John, R.; Chen, J.; Xiao, J.; Amirkhiz, R.G.; Giannico, V.; Kussainova, M. Optimal ranges of social-environmental drivers and their impacts on vegetation dynamics in Kazakhstan. *Sci. Total Environ.* **2022**, *847*, 157562. [CrossRef]

62. Zhang, Y.; Jiang, X.; Lei, Y.; Gao, S. The contributions of natural and anthropogenic factors to NDVI variations on the Loess Plateau in China during 2000–2020. *Ecol. Indic.* **2022**, *143*, 109342. [CrossRef]

63. Mehri, A.; Salmanmahiny, A.; Tabrizi, A.R.M.; Mirkarimi, S.H.; Sadoddin, A. Investigation of likely effects of land use planning on reduction of soil erosion rate in river basins: Case study of the Gharesoo River Basin. *Catena* **2018**, *167*, 116–129. [CrossRef]

64. Kumar, R.; Nath, A.J.; Nath, A.; Sahu, N.; Pandey, R. Landsat-based multi-decadal spatio-temporal assessment of the vegetation greening and browning trend in the Eastern Indian Himalayan Region. *Remote Sens. Appl. Soc. Environ.* **2022**, *25*, 100695. [CrossRef]

65. Wang, X.; Wu, J.; Liu, Y.; Hai, X.; Shanguan, Z.; Deng, L. Driving factors of ecosystem services and their spatiotemporal change assessment based on land use types in the Loess Plateau. *J. Environ. Manag.* **2022**, *311*, 114835. [CrossRef] [PubMed]

66. Beyaztas, U.; Salih, S.Q.; Chau, K.-W.; Al-Ansari, N.; Yaseen, Z.M. Construction of functional data analysis modeling strategy for global solar radiation prediction: Application of cross-station paradigm. *Eng. Appl. Comp. Fluid* **2019**, *13*, 1165–1181. [CrossRef]